Electronic Supplementary Information

Transformation of Clinical Waste into Heteroatom-Doped Porous Carbon Materials Towards a Highly Efficient Energy Storage Device

Siddheswar Rudra,† Soubhik De,† and Debabrata Pradhan*

Materials Science Centre, Indian Institute of Technology, Kharagpur 721 302, W. B., India

*E-mail: deb@matsc.iitkgp.ac.in

† Equally contributed

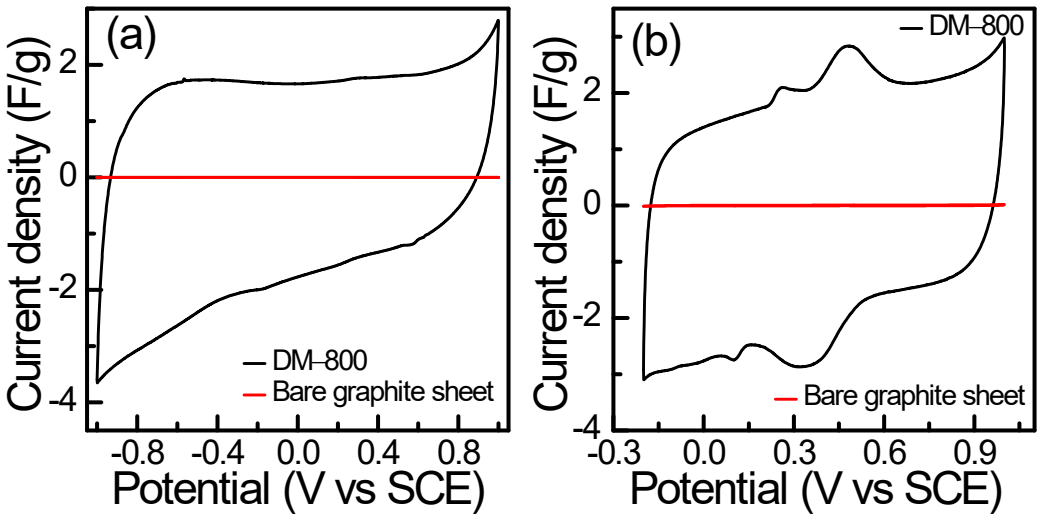

Fig. S1. Cyclic voltammograms of the synthesized porous carbon materials (i.e., DM-800) and bare graphite sheet at a scan rate of 10 mV/s in (a) neutral and (b) acidic electrolytes.

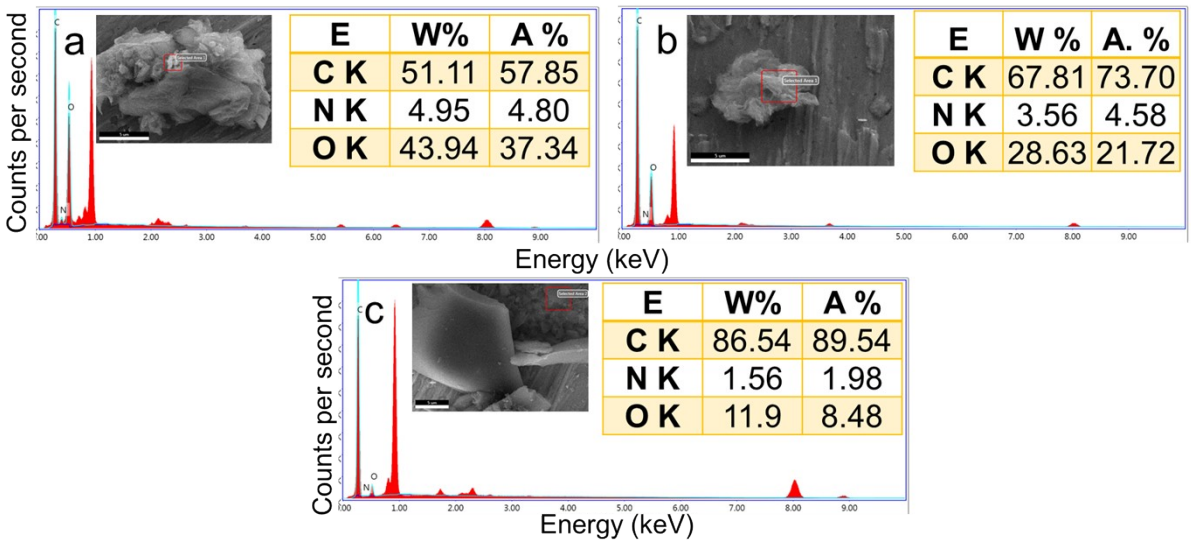

Fig. S2. Energy-dispersive spectra of the synthesized carbon materials derived from DMs, (a) DMW, (b) DM-700, and (c) DM-850.

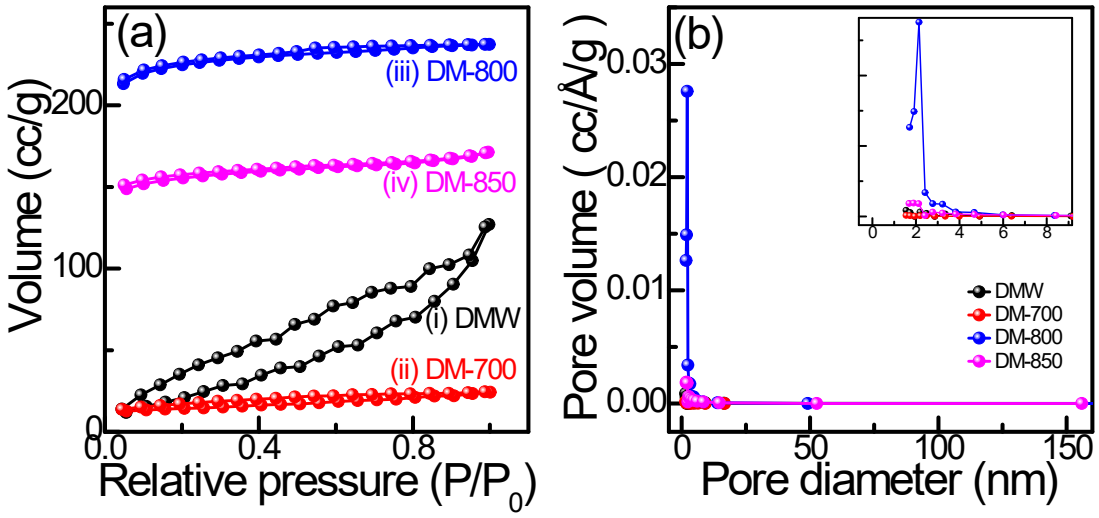

Fig. S3. (a) N_2 adsorption-desorption isotherms and (b) Pore size distributions of the synthesized porous carbon materials, i.e., DMW, DM-700, DM-800, and DM-850.

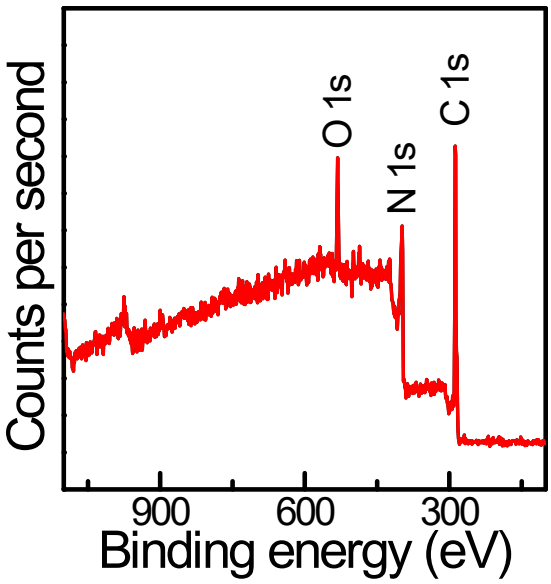

Fig. S4. Survey XPS spectrum of DM-800.

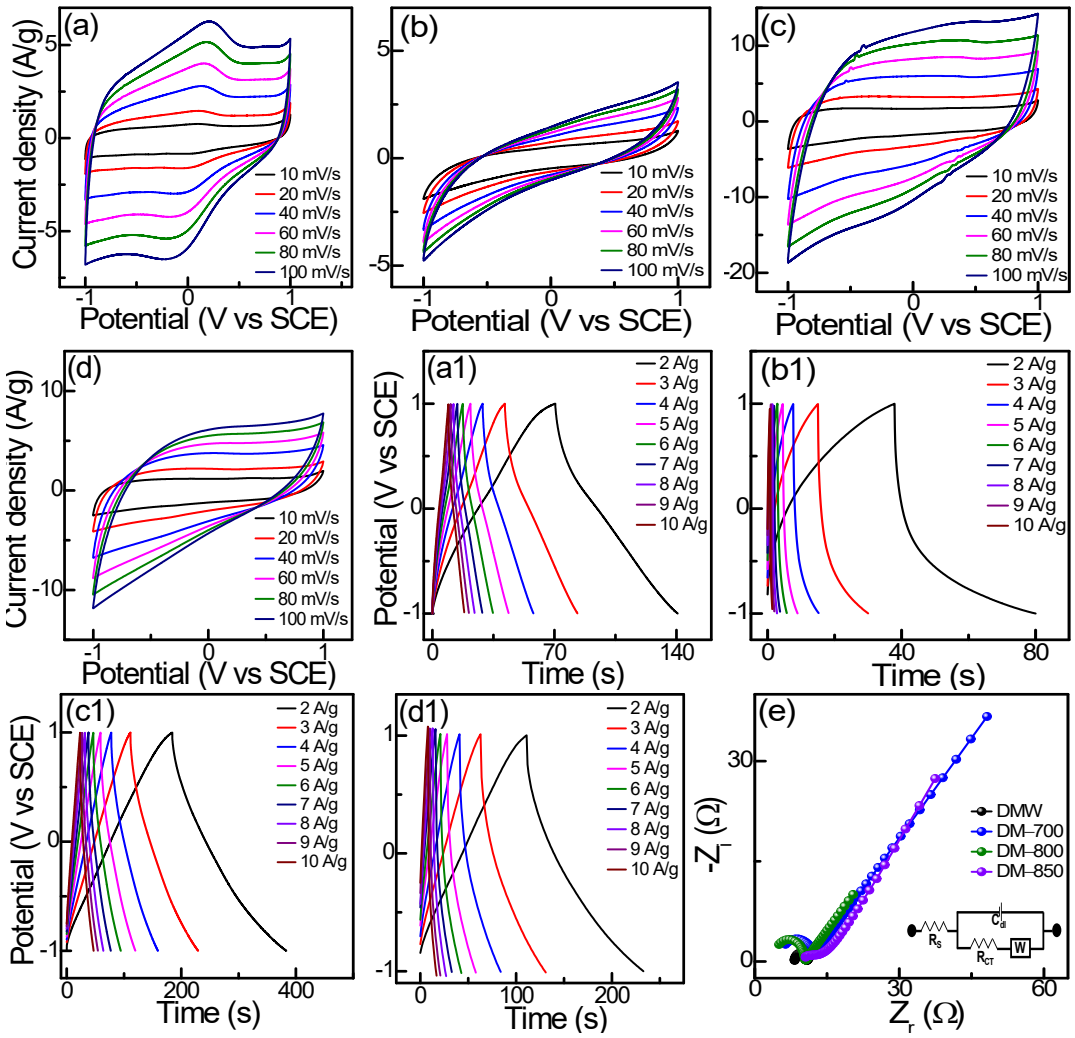

Fig. S5. (a-d) CV profiles at different scan rates (mV/s), (a1-d1) GCD curves at different current densities (A/g), (e) EIS plots of the synthesized porous carbon materials, i.e., (a,a1) DMW, (b,b1) DM-700, (c,c1) DM-800, and (d,d1) DM-850 in a neutral (0.5 M Na_2SO_4) electrolyte using three-electrode configuration.

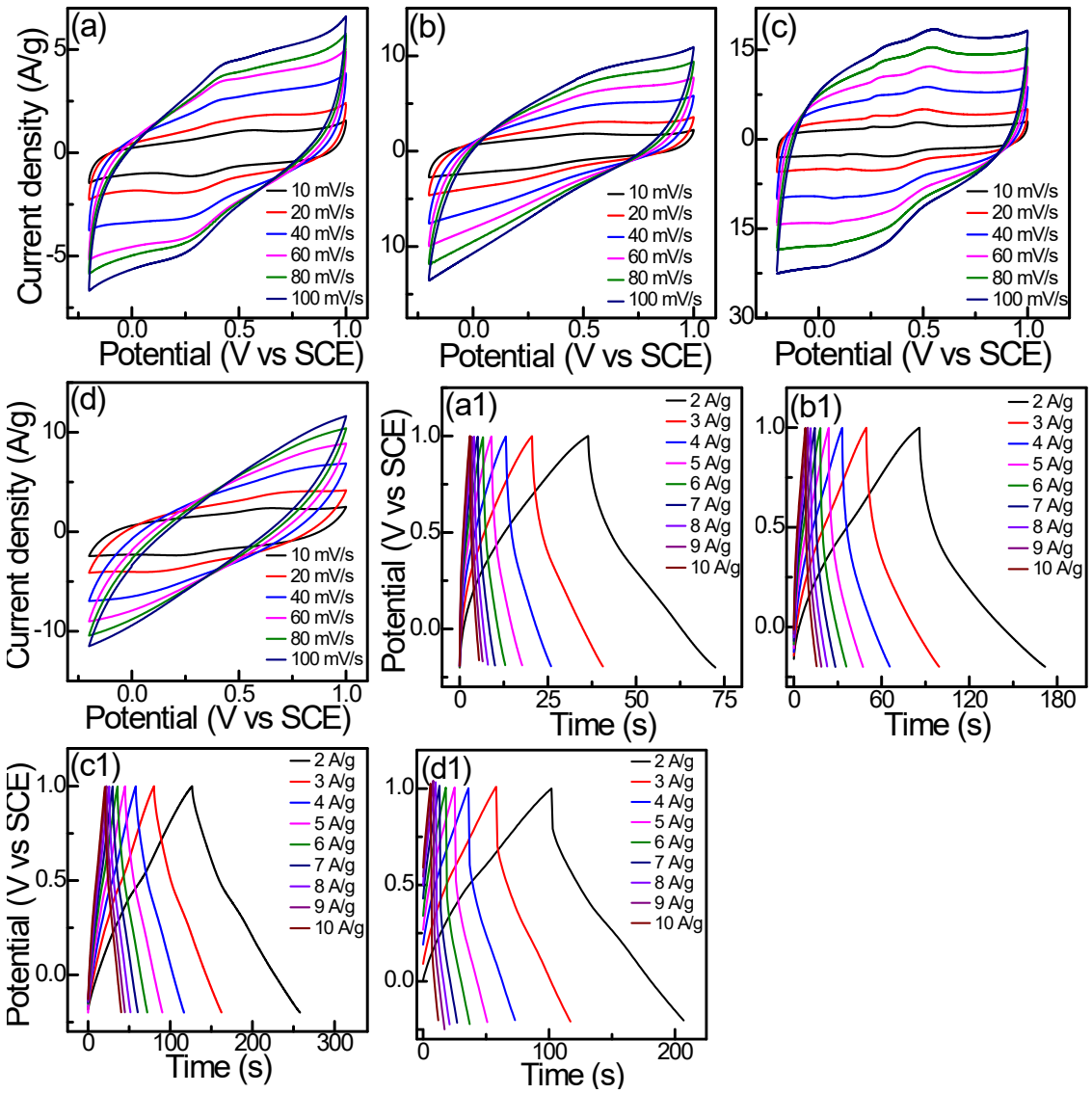

Fig. S6. (a-d) CV profiles at different scan rates (mV/s), (a1-d1) GCD curves at different current densities (A/g), i.e., (a,a1) DMW, (b,b1) DM-700, (c,c1) DM-800, and (d,d1) DM-850 in an acidic (0.5 M H_2SO_4) electrolyte using three-electrode configuration.

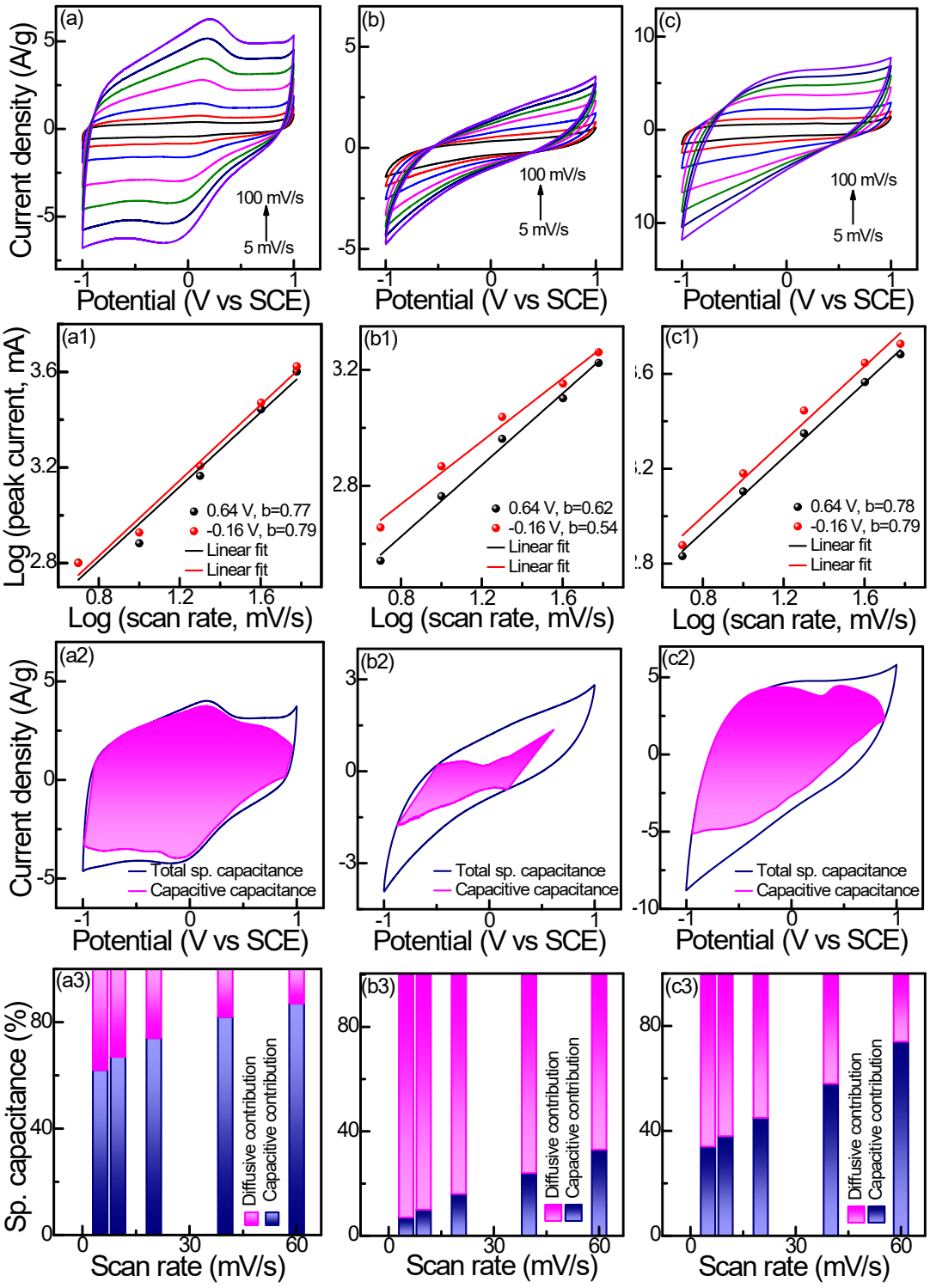

Fig. S7. (a-c) CV curves at different scan rates, (a1-c1) logarithmic plot of peak current vs. scan rates, (a2-c2) capacitive and diffusive contribution plots at constant scan rate of 60 mV/s, and (a3-c3) Bar diagram of specific capacitance contributions at different scan rates of the synthesized carbon materials, i.e., (a,a1,a2,a3) DMW, (b,b1,b2,b3) DM-700, and (c,c1,c2,c3) DM-850 in a neutral (0.5 M Na_2SO_4) electrolyte.

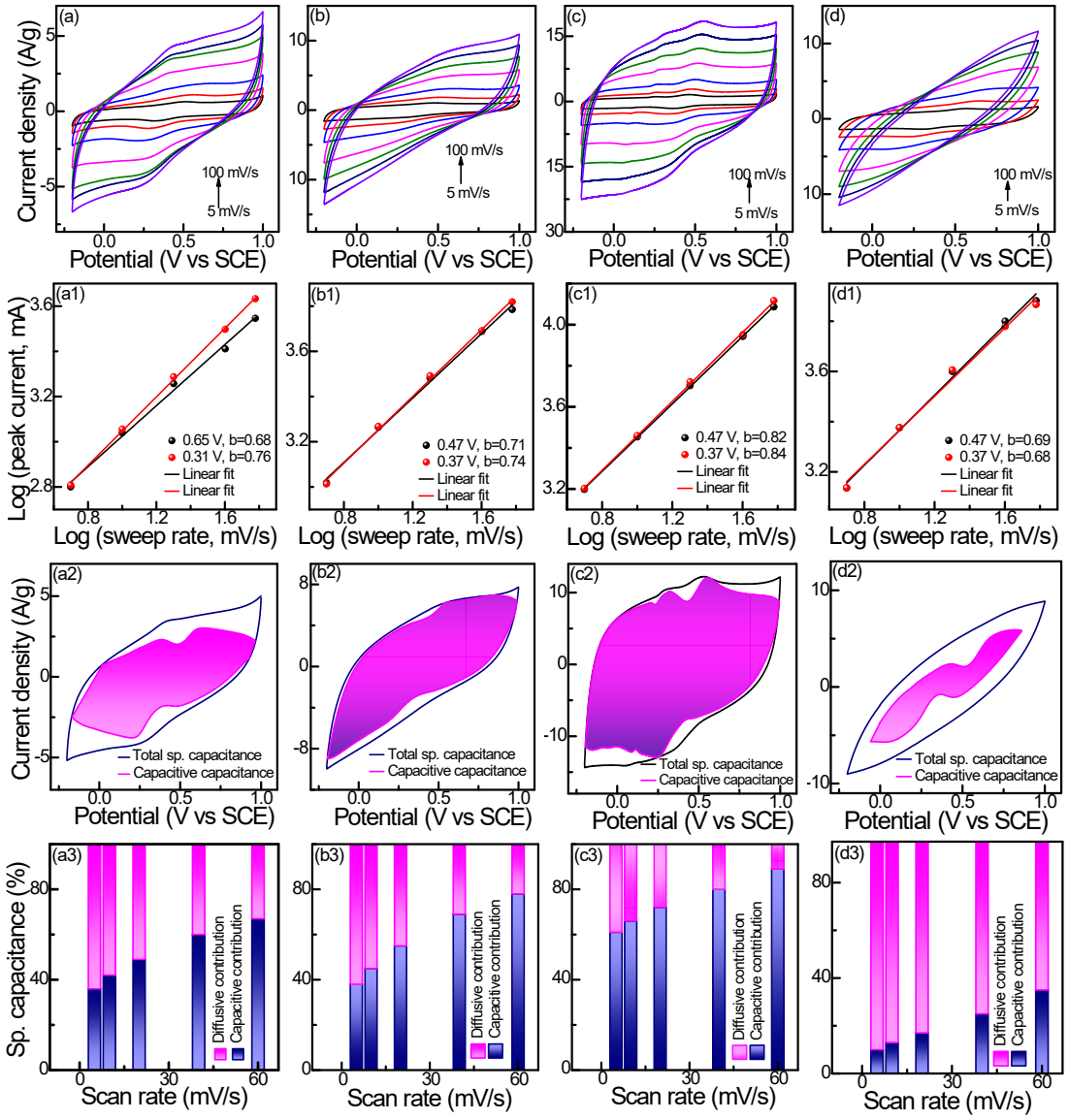

Fig. S8. (a-d) CV curves at different scan rates, (a1-d1) logarithmic plot of peak current at different scan rates, (a2-d2) capacitive and diffusive contribution plot at constant scan rate of 60 mV/s, and (a2-d3) Bar diagram of specific capacitance contributions at different scan rates of the synthesized carbon materials, i.e., (a,a1,a2,a3) DMW, (b,b1,b2,b3) DM-700, (c,c1,c2,c3) DM-800, and (d,d1,d2,d3) DM-850, in an acidic (0.5 M H_2SO_4) electrolyte.

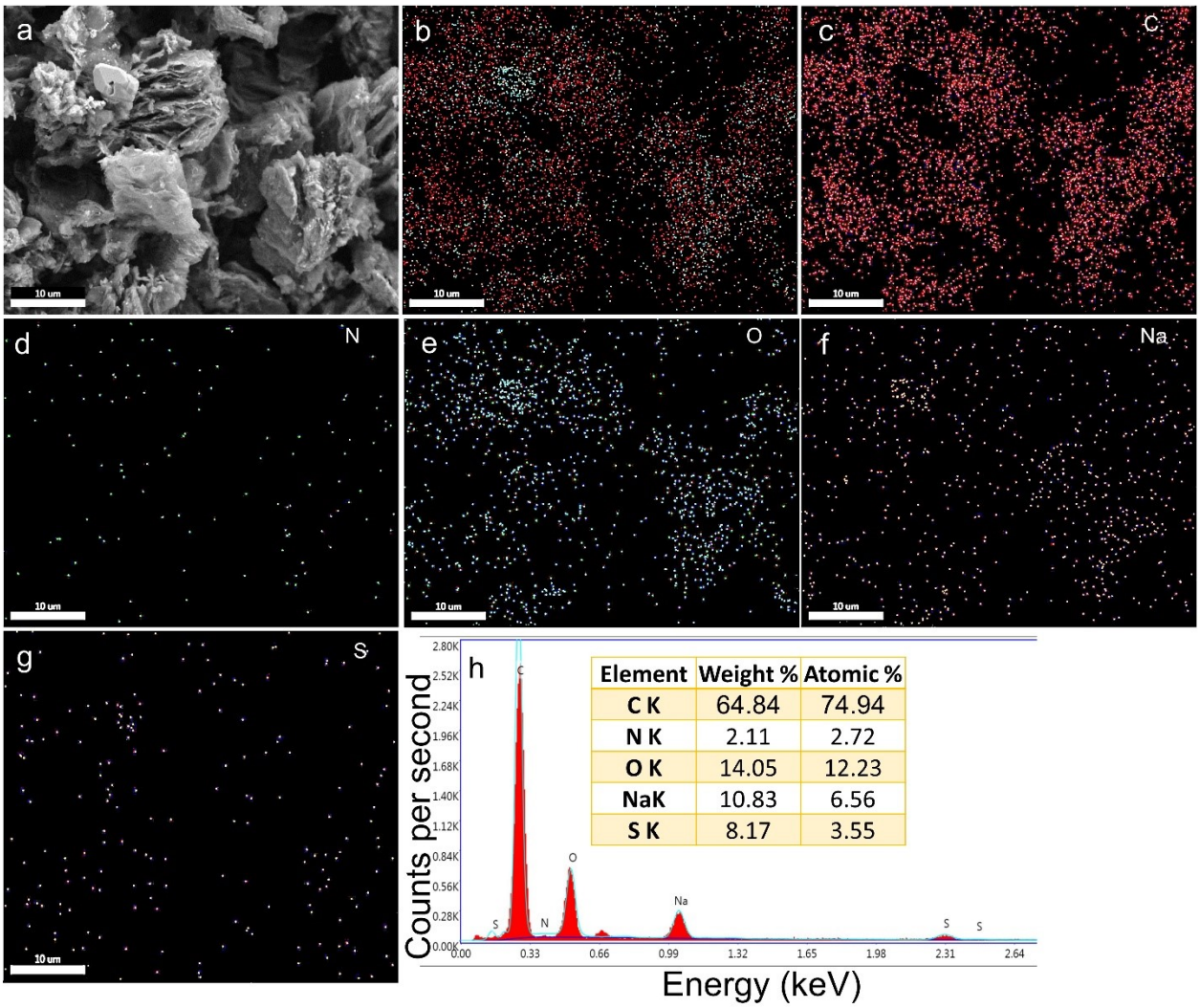

Fig. S9. (a) FESEM image, and the elemental mapping of DM-800 after galvanic charging in a neutral (0.5 M Na_2SO_4) electrolyte, (b) all element overlay, and specific elemental distribution of (c) C, (d) N, (e) O, (f) Na, (g) S, and (h) EDX spectrum.

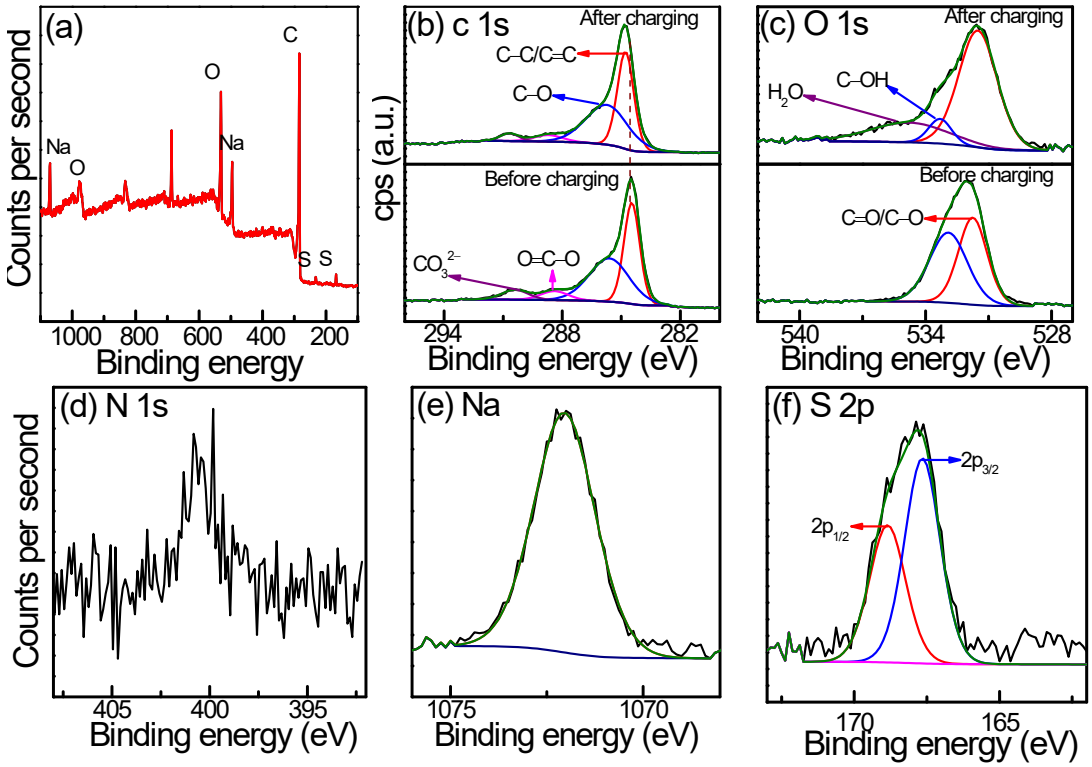

Fig. S10. (a) Survey XPS spectrum and (b) C 1s, (c) O 1s, (d) N 1s, (e) Na 1s, (f) S 2p high-resolution XPS spectrum of DM-800 after galvanic charging in neutral (0.5 M Na_2SO_4) electrolyte.

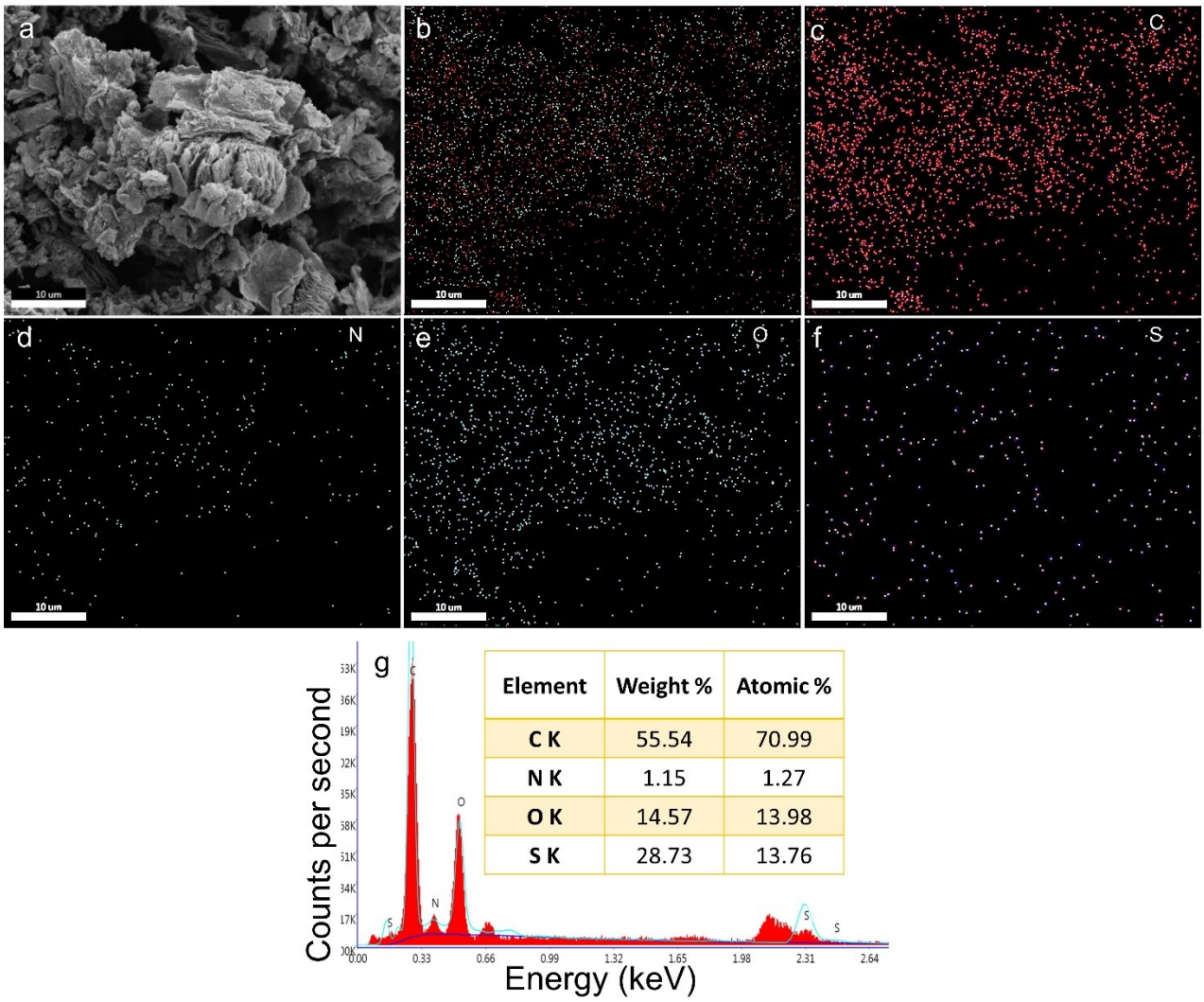

Fig. S11. (a) FESEM image, and the elemental mapping of DM-800 after galvanic charging in acidic (0.5 M H_2SO_4) electrolyte (b) all element overlay, and specific elemental distributions of (c) C, (d) N, (e) O, (f) S, and (g) EDX spectrum.

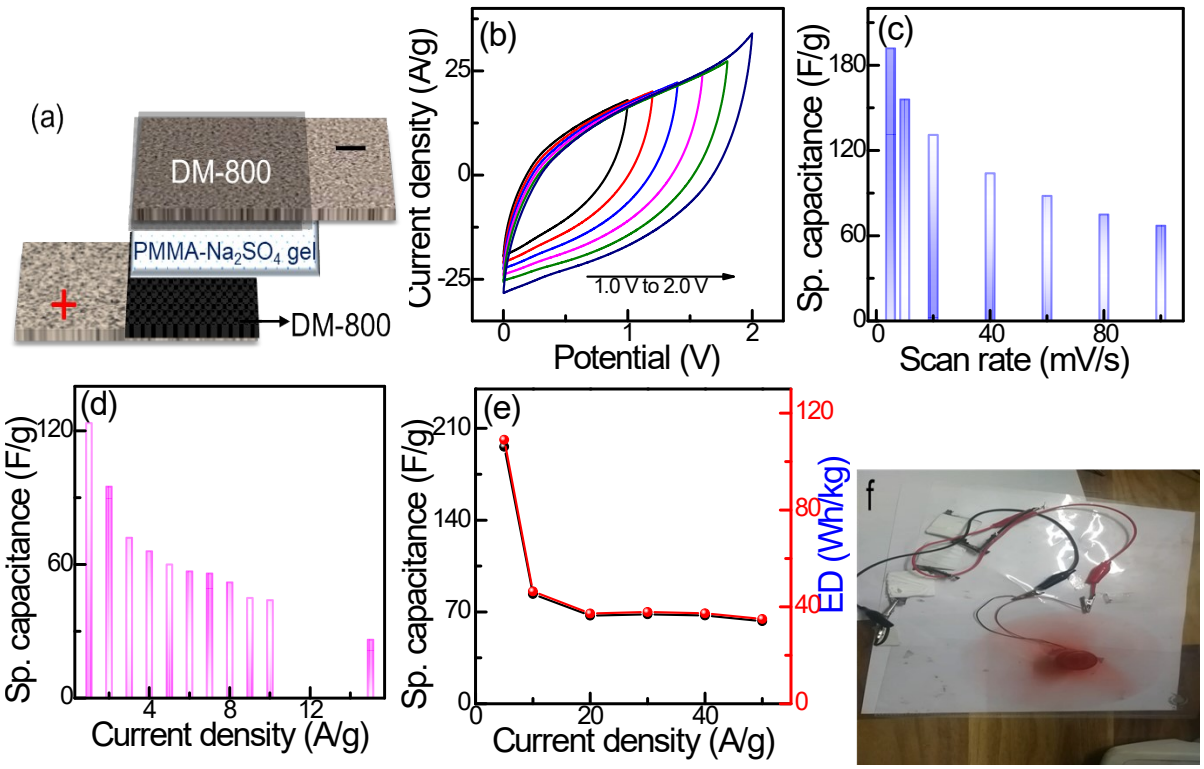

Fig. S12. (a) Schematic representation of the fabricated solid-state symmetric device using DM-800 as the electrodes and PMMA-Na_2SO_4 as a gel electrolyte. (b) CV curves at various potential windows at a scan rate of 100 mV/s, (c) Specific capacitance at different scan rates, (d) Specific capacitance at different current densities (A/g), (e) Specific capacitance and ED at different current densities with a lower discharging rate (0.25 A/g), (f) Real application demonstration using a motorized fan of the fabricated solid-state symmetric device.

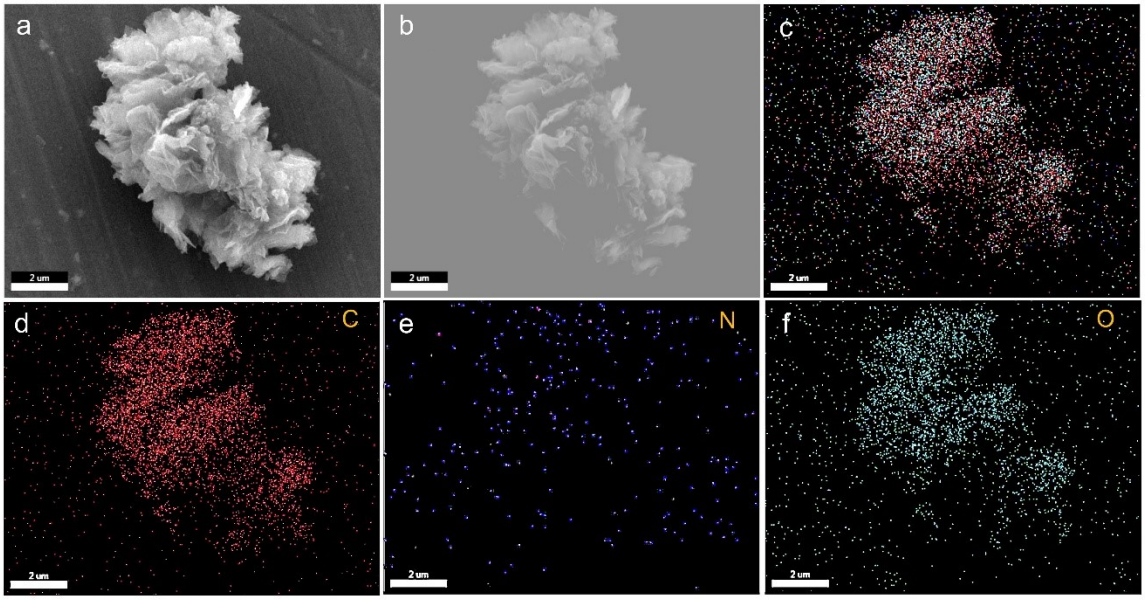

Fig. S13. (a,b) FESEM images, and the elemental mapping of DM-800 after cycle stability, (c) all element overlay, and specific elemental distributions of (d) C, (e) N, and (f) O.

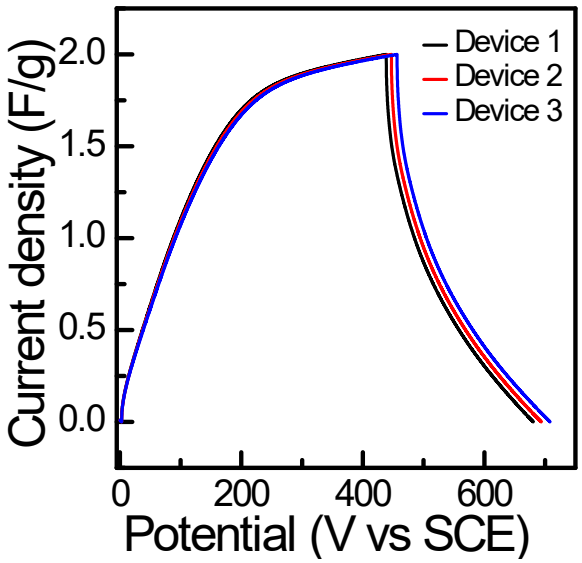

Fig. S14: The GCD curves at the current density of 1A/g of three devices fabricated using DM-800.

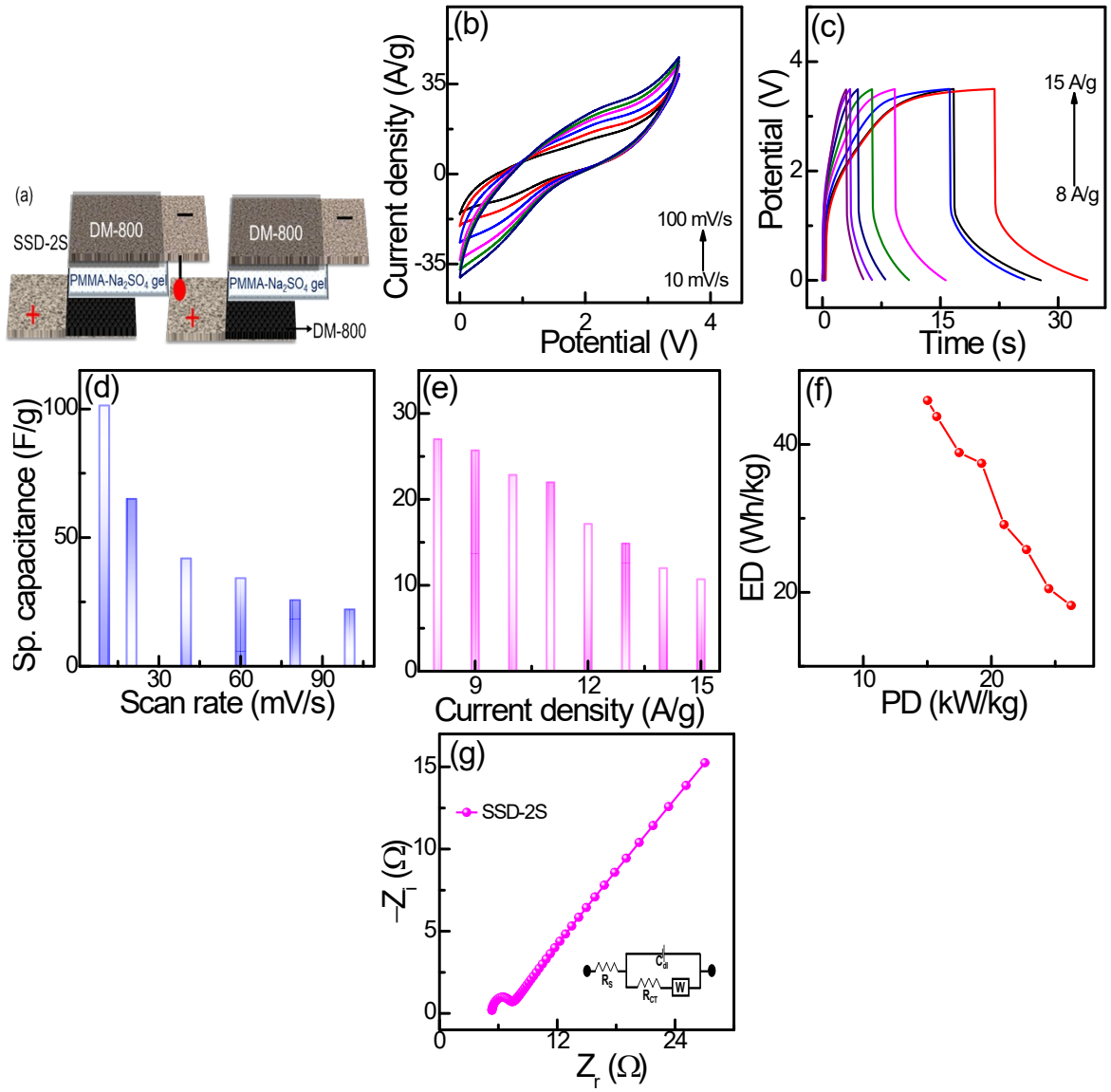

Fig. S15. (a) Schematic representation of the two fabricated solid-state symmetric devices in series connection (SSD-2S). (b) CV curves at different scan rates (mV/s), (c) GCD curves at different current densities (A/g), (d) Specific capacitance vs scan rates plot, (e) Specific capacitance vs current densities plot, (f) Ragone plot, (g) EIS spectrum (inset represents equivalent circuit) of the fabricated device SSD-2S.

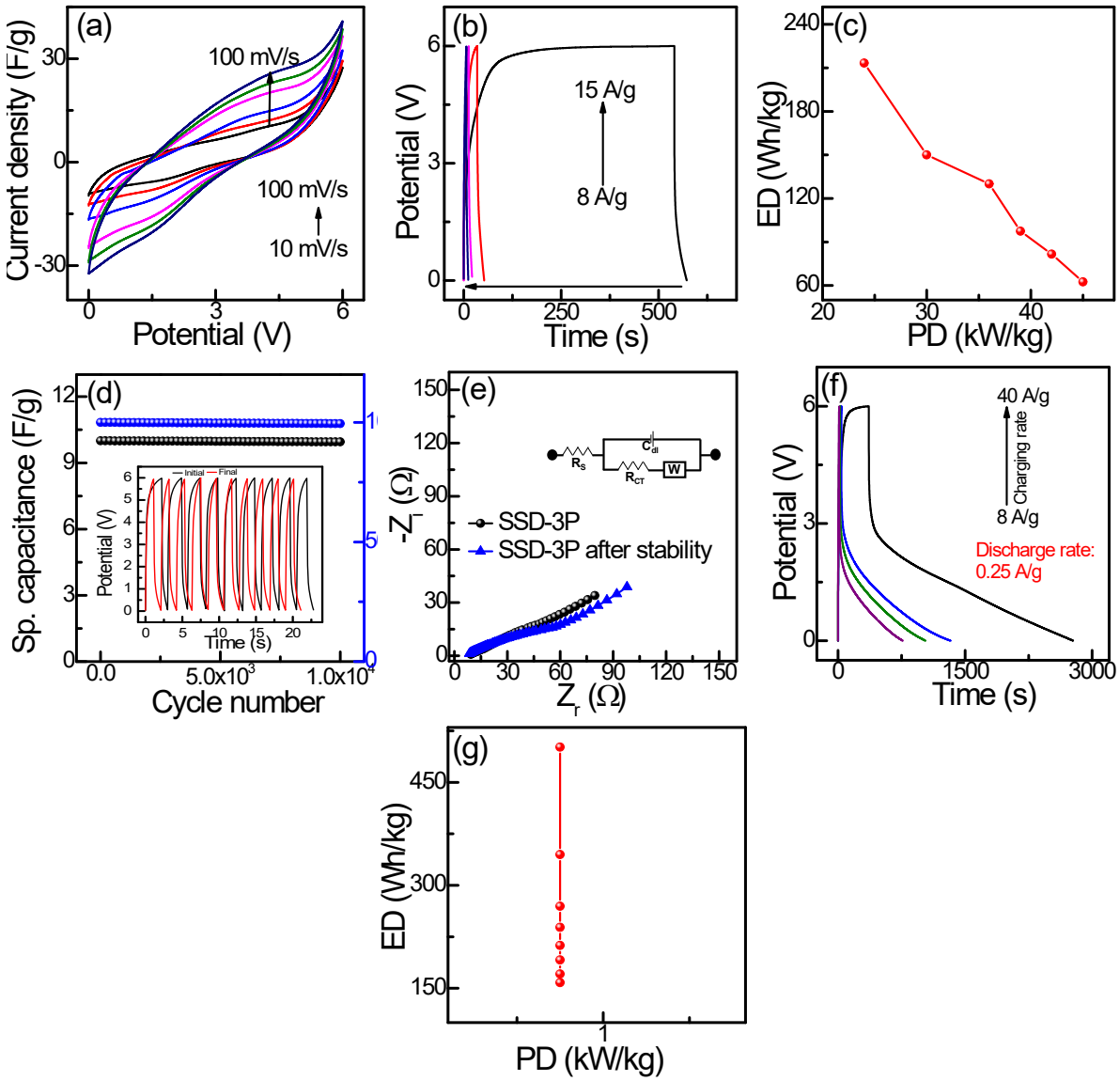

Fig. S16. (a) CV curves of the three fabricated solid-state symmetric devices in series connection (SSD-3S), (b) GCD curves at different current densities (A/g), (c) Ragone plot, (d) durability test upto 10,000 continuous charge-discharge cycles, (e) EIS spectra before and after stability (inset represents equivalent circuit), (f) GCD curves with different charging rate (A/g) and constant discharging rate, (g) Ragone plot.

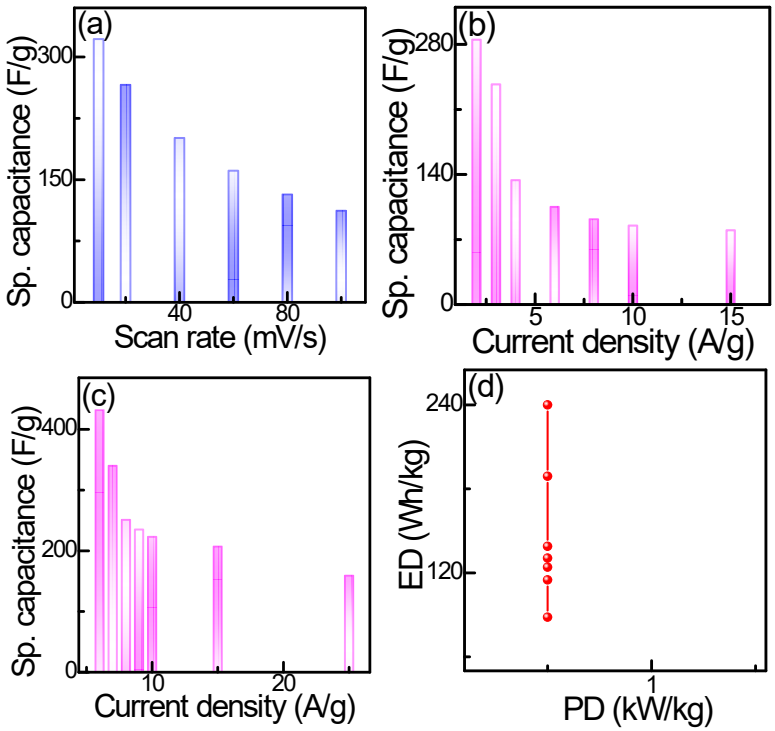

Fig. S17. (a) Specific capacitance vs different scan rates plot, (b) Specific capacitance vs current densities plot, (c) Specific capacitance vs current densities plot at variable charging rate with constant discharging rate, (d) Ragone plot of the fabricated SSD-3P device.

Table S1. Comparison of energy storage performance of recently reported porous carbon materials in the symmetric devices.

Carbon source	*Activation agent*	*Electrolyte*	*Specific capacitance (F/g)*	*Stability*	*ED (Wh/kg)*	*PD (kW/kg)*	*Ref.*
Furfural residue	H_3PO_4, KOH, Melamine	6 M KOH	337 at 0.5 A/g	100 %	11.81	0.275	[1]
Bambyx mori silk	Melamine, $KHCO_3$	6 M KOH	204 at 1 A/g	100 %	10.9	0.350	[2]
Lignin	KOH	6 M KOH	350 at 1 A/g	97.2 %	10.17	0.125	[3]
Sawdust	H_3PO_4	1 M H_2SO_4	169 at 0.5 A/g	98.3 %	10.6	0.2248	[4]
Waste durian peels	$KHCO_3$	6 M KOH	267 at 1 A/g	93.3 %	14.45	0.225	[5]
Enzymatic hydrolysis lignin	KOH	6 M KOH	254 at 0.2 A/g	83 %	6.3	3.4	[6]
Diapers	KOH	6 M KOH	353 at 1 A/g	87.65%	7.22	0.125	[7]
Mango kernel	-	3 M KOH	206 at 0.25 A/g	100 %	12.32	5.137	[8]
Montmorillonite	KCl	6 M KOH	232 at 0.5 A/g	98.5 %	4.81	0.05	[9]
Disposable face mask (DM)	-	1 M Na_2SO_4/ 0.5 M H_2SO_4	372/282 at 1 A/g	98 %	68.61	15.00	This work

References

[1] F. Liu, F. Zhang and J. Niu, *RSC Adv.*, 2025, **15**, 2582–2590.

[2] V. Molahalli, V. S. Bhat, A. Sharma, G. Soman and G. Hegde, *RSC Adv.*, 2025, **15**, 14183–14193.

[3] G. Song, Y. Tian, J. Wang, S. Zhang, H. Hou, C. Wei, L. Cao, J. Zhang and S. Zhang, *RSC Adv.*, 2025, **15**, 20657–20667

[4] H. Wang, F. Xiong, F. Guo, Y. Han, F. Chen, B. Ma, J. Yang, M. Wen, Y. Qing, F. Chu and Y. Wu, *Colloids Surfaces A Physicochem. Eng. Asp.*, 2022, **655**, 130237.

[5] G. Singh, R. Bahadur, A. M. Ruban, J. M. Davidraj, D. Su and A. Vinu, *Green Chem.*, 2021, **23**, 5571–5583.

[6] Z. Ding, T. Lei, L. Dong, C. Pan, R. Wang, G. Pang and S. Ren, *Biomass and Bioenergy*, 2025, **194**, 107688.

[7] L. Li, J. Wen, J. Liang, X. Cheng, J. Yao, Y. Gao, S. Hu, H. Wu, J. Zheng and G. Li, *Chem. - A Eur. J.*, 2025, **31**, e202404569.

[8] L. Wang, Q. Zhang, X. Yao, J. Bai, T. Zhou, C. Dong, J. Wu and Y. Zhang, *J. Power Sources*, 2025, **630**, 236079.

[9] G. Lin, Q. Wang, X. Yang, Z. Cai, Y. Xiong and B. Huang, *RSC Adv.*, 2020, **10**, 17768–17776.